

DAC-Less and DSP-Free 112 Gb/s PAM-4 Transmitter Using Two Parallel Electroabsorption Modulators

Jochem Verbist¹, Joris Lambrecht¹, Michiel Verplaetse¹, Joris Van Kerrebrouck¹, Ashwyn Srinivasan, Peter De Heyn, Timothy De Keulenaer, Xin Yin², Guy Torfs², Joris Van Campenhout², Gunther Roelkens², and Johan Bauwelinck²

(Post-Deadline Paper)

Abstract—Four-level pulse amplitude modulation (PAM-4) is widely regarded as the modulation format of choice for the next generation of 400 gigabit Ethernet short-reach optical transceiver. However, generating and receiving PAM-4 at line rates of 112 Gb/s has proven challenging, without relying on power-hungry tools as digital signal processing and digital-to-analog converters, as it requires linearity from the E/O-components in the link and/or predistortion techniques. Moving the binary to multilevel conversion to the optical domain would greatly relax these requirements. Electroabsorption-based transceivers would be ideally suited for this type of data center interconnects as they are capable of combining low-power and high bandwidth operation with a very compact layout, removing the need for large travelling wave structures and dedicated 50 Ω terminations. In this paper, we present a novel transmitter topology for generating PAM-4 using two binary-driven electroabsorption modulators in parallel. Using this approach, we achieve superior performance with respect to a single, but identical multilevel-driven EAM. Finally, we demonstrate the first silicon-based modulator capable of transmitting single-lane 112 Gb/s PAM-4 over 2 km of standard single-mode fiber without any electrical digital-to-analog converter, DSP, or long transmission line structures and terminations.

Manuscript received November 12, 2017; revised December 18, 2017; accepted December 21, 2017. Date of publication January 2, 2018; date of current version March 1, 2018. This work was partially supported in part by IMEC's industry-affiliation R&D program on Optical I/O, the UGent BOF GOA Research Fund, the Research Foundation Flanders (FWO), FWO-SBO, and the H2020 project TERABOARD. (Corresponding author: Jochem Verbist.)

J. Verbist is with the Ghent University—IMEC, IDLab, Department of Information Technology, Ghent 9052, Belgium. He is also with the Ghent University—IMEC, Photonics Research Group, Department of Information Technology, Ghent 9052, Belgium (e-mail: jochem.verbist@ugent.be).

J. Lambrecht, M. Verplaetse, J. Van Kerrebrouck, X. Yin, G. Torfs, and J. Bauwelinck are with the Ghent University—IMEC, IDLab, Department of Information Technology, Ghent 9052, Belgium (e-mail: joris.lambrecht@ugent.be; michiel.verplaetse@ugent.be; joris.vankerrebrouck@ugent.be; xin.yin@ugent.be; guy.torfs@ugent.be; johan.bauwelinck@ugent.be).

G. Roelkens is with Ghent University—IMEC, Photonics Research Group, Department of Information Technology, Ghent 9052, Belgium (e-mail: gunther.roelkens@ugent.be).

A. Srinivasan, P. De Heyn and J. Van Campenhout are with the IMEC, Leuven 3001, Belgium (e-mail: ashwyn.srinivasan@imec.be; Peter.DeHeyn@imec.be; joris.vancampenhout@imec.be).

T. De Keulenaer is with BiFAST, Ghent 9000, Belgium (e-mail: timothy@bifast.io).

Color versions of one or more of the figures in this paper are available online at <http://ieeexplore.ieee.org>.

Digital Object Identifier 10.1109/JLT.2017.2789164

Index Terms—Electro-absorption modulators, modulation, PAM-4, short-reach interconnects, silicon photonics.

I. INTRODUCTION

NEXT generation transceivers for short-reach optical interconnects will likely employ a four lane scheme with 100G line rates [1], as this is a natural successor of the 100 Gigabit Ethernet (GbE) modules used today without having to increase the component and lane count and, as such, the packaging cost. Although some demonstrations of 100G line rates using non-return to zero (NRZ) or 3-level duobinary exist [2]–[6], four-level pulse amplitude modulation (PAM-4) has emerged as the preferred modulation format for this scenario, balancing relaxed bandwidth requirements with increased complexity for the E/O-components in the link. Currently, most of the PAM-4 transmitters at 100 Gb/s and above still require electrical digital-to-analog converters (DACs) to generate the multilevel signal [7], [8]. However, to drive a single optical modulator the DAC must provide a sufficiently large voltage swing or must be followed by a linear output driver. Both options substantially increase the power consumption of the transmitter with respect to a conventional NRZ driver at the same baud rate. Moving the DAC-operation to the optical domain would remove the linearity requirements at the transmitter, reducing the complexity of the electrical front-end and its power consumption. Recently, several optical DACs have been proposed using a segmented Mach-Zehnder modulator (MZM) [9], parallel MZMs [10], [11], silicon ring modulators [12], [13], Si-on-IIIIV electroabsorption modulated distributed feedback laser (EML DFB) [14] or by using polarization division multiplexing (PDM) for the least and most significant bit (LSB and MSB) [15], [16]. Although the MZM-based solutions show good performance, they might not be suited for short-reach interconnects as they typically require large transmission line structures and dedicated, power-consuming terminations. Silicon microring modulators have been used [12], [13], but current demonstrations are limited to 80 Gb/s even with DSP at the transmitter and receiver side. Furthermore, ring resonators are very susceptible to temperature variations and need control systems to guarantee stable operation. In [14], direct and external modulation of a

III-V-on-Si DFB laser were combined to encode the LSB and the MSB. However, the speed was limited to 50 Gb/s PAM-4 as the bandwidth of the direct modulation (14 GHz) was a bottleneck for the overall data rate. Another approach towards a DAC-less transmitter was shown in [15], [16], where a PDM scheme was used to transport the LSB and MSB over the optical channel with an electro-absorption modulated laser in Indium Phosphide (InP). This allows for an independent power addition at the receiver, provided it is polarization insensitive. A drawback of this method is that it already occupies both polarizations, removing the possibility of doubling the data rate by implementing a PDM scheme. Moreover, the demonstrations still rely on discrete external components to perform the polarization handling as these are not readily available in an InP integration platform. Implementing a compact, low-power 112 Gb/s PAM-4 transmitter in a Silicon platform would provide a low-cost solution, which could be produced in high volume leveraging the existing CMOS fabrication infrastructure.

In this paper we present a novel single-lane, single-polarization integrated PAM-4 transmitter based on the vector addition of two binary driven amplitude modulators in parallel. An integrated prototype consisting of two compact, waveguide GeSi electro-absorption modulators (EAMs) was fabricated in imec's Silicon Photonics platform, outperforming a single multilevel driven GeSi EAM. Using this prototype, we demonstrate the first transmission of 112 Gb/s PAM-4 over 2 km of standard single mode fiber with a silicon-based modulator without any DAC, DSP or large transmission line structures. This paper is an invited extension of our post deadline paper presented at ECOC 2017 [17].

II. PROPOSED TOPOLOGY

As the transfer function of an electro-absorption modulator is typically non-linear and not symmetrical (as is the case for a MZM), generating a clean PAM-4 signal with equidistant levels on a single EAM can be challenging. Often, a power-hungry DAC or some clever analog pre-distortion method is required to produce equidistant eye levels. This becomes especially difficult if the EAM has only limited extinction ratio ($ER < 10$ dB). Performing the multilevel generation in the optical domain rather than the electrical domain by operating the EAMs as two binary driven switches, allows us to bypass the non-linearity of the modulator. More importantly, this also eliminates the need for a DAC or linear driver at the transmitter, allowing simple and low-power NRZ driver topologies (e.g., CMOS inverters) to be used instead. In other words, the linearity requirement is completely removed from the transmit side in both the electrical and optical domain.

Here, we present a new type of optical DAC using 2 identical, binary driven EAMs in parallel. Although we have focused on EAMs as modulators to implement the proposed optical DAC topology, any type of amplitude modulator can be used. As such, all the principles and remarks that are discussed in the following paragraphs, also apply to any choice of amplitude modulator.

A. Principle of Operation

The proposed modulator is shown in Fig. 1 and consists of a splitter with power ratio $\alpha:1-\alpha$, two identical EAMs, a DC

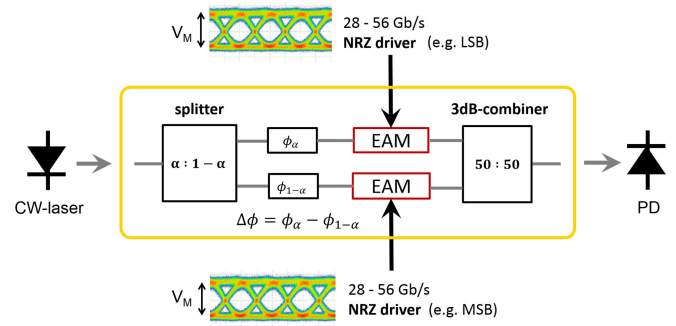


Fig. 1. Generalized block diagram of the PAM-4 generation topology using 2 binary driven, parallel electro-absorption modulators as proposed in this work. Although the block diagram uses EAMs, this topology will work for any type of amplitude modulator.

phase shifter and a 3 dB-combiner. The DC phase shift $\Delta\phi$ between both arms is needed to provide an additional degree of freedom to place the PAM-4 levels equidistantly. The input splitter can be realized as a tunable splitter (e.g., Mach-Zehnder Interferometer, using commonly available components such as 1×2 and 2×2 multi-mode interferometers) or as a custom design (e.g., a star coupler with fixed coupling ratio). When branch α corresponds to the LSB and branch $1-\alpha$ to the MSB, the output power levels P_{ij} are given by

$$P_{ij} = \frac{1}{2} \left| \sqrt{\frac{1-\alpha}{IL \cdot ER^{(1-i)}}} + e^{j\Delta\phi} \sqrt{\frac{\alpha}{IL \cdot ER^{(1-j)}}} \right|^2 \quad \text{for } i, j = 0, 1 \quad (1)$$

Where $\{i, j\} = \{\text{MSB}, \text{LSB}\}$ and the (identical) EAMs are characterized by a bias and voltage dependent ER and insertion loss (IL). For simplicity, we assume that no phase difference is introduced between the 0 and the 1 level by the EAMs. By choosing an appropriate α , we can fix the levels where at least one EAM is absorbing (i.e., the symbols 00, 01 and 10) at an equidistant position. However, when both EAMs are transparent (i.e., generating 11) this level will always be above its equidistant position due to the cross product of both terms in (1). Adding a phase shift $\Delta\phi$ gives us an additional degree of freedom to place the 11-symbol at its equidistant position as P_{11} becomes:

$$P_{11} = \frac{1}{2IL} \left[1 + 2\sqrt{(1-\alpha)\alpha} \cos(\Delta\phi) \right] \quad (2)$$

B. Special Case: $\alpha = 1/3$ and $\Delta\phi = 90^\circ$

A particularly interesting solution is found, when we choose $\alpha = 1/3$ and $\Delta\phi = 90^\circ$, for which the vector diagram representing the on- and off- states of each EAM is depicted in Fig. 2. In this example, the red vectors correspond to EAMs with no IL and an ER of 10 dB. This configuration has the special property that any given combination of $\{ER, IL\}$ generates equidistant PAM-4 levels, as long as the EAMs are identical. This can be understood by realizing that both basis vectors are affected proportionally, i.e., for any choice of $\{ER, IL\}$ the points $(\sqrt{P_{00}}, \sqrt{P_{10}}, \sqrt{P_{11}})$ always form a similar triangle, for which the ratio of its sides remains the same.

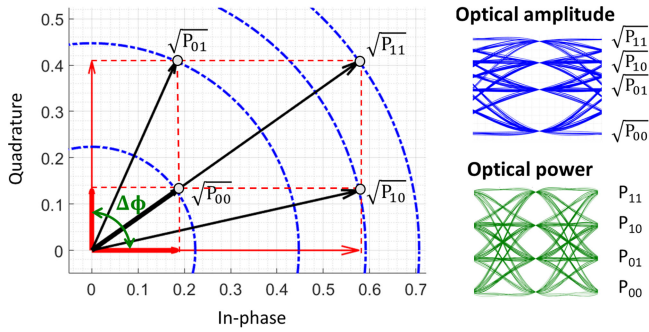


Fig. 2. Example of an equidistant PAM-4 generation scheme, using the first quadrant of the complex plane, for the special case that the power split ratio is chosen 0.33:0.66 and the phase $\Delta\phi$ between the branches is 90° . The red arrows represent the on- and off-state of the 2 EAMs, when driven separately. They form the basis vectors for the PAM-4 generation. The limited extinction ratio (10 dB in this example) and the resulting non-perfect zero level, is represented by the bold vectors. The 4 black vectors representing the 4 constellation points ($\sqrt{P_{00}}$, $\sqrt{P_{01}}$, $\sqrt{P_{10}}$, $\sqrt{P_{11}}$) are found by the vector addition of each state (on/off) of both basis vectors. Squaring the moduli of these 4 vectors gives us the power levels of the PAM-4 signal, when received by a square-law photodiode.

A drawback of this shaping with $\alpha = 1/3$ and $\Delta\phi = 90^\circ$ is that the optical swing is 3 dB less than what can be maximally achieved with a single multilevel driven modulator for the same average input power, assuming full use of the available extinction by proper placement of the electrical PAM-4 levels. Nevertheless, we will demonstrate in Section IV that for modulators with a limited ER and non-linear transfer function, this penalty will be more than compensated by the improvement in eye quality.

C. PAM-4 Shaping by Vector Addition

Not only equidistant eyes can be obtained, but also shaped eyes (i.e., pre-distorted) can be achieved by altering the split ratio, the phase or both. Fig. 3 shows an examples of varying the phase (Fig. 3(b)) or the split ratio (Fig. 3(c)) with respect to the special configuration as discussed above (Fig. 3(a)). Equidistant eyes are not necessarily the best configuration to obtain the minimal bit error ratio (BER) using this type of transmitter, as will be discussed next.

Choosing $\Delta\phi = 0^\circ$, we lose the equidistance of the power levels but the total swing of the PAM-4 eye almost doubles, reducing this shaping IL to only 0.13 dB. Interestingly, while the bottom and especially the top eye height increases when compared to Fig. 3(a), the eye height of the middle eye remains identical. Thus, if the receiver is not limited by its dynamic range, the top eye will only contribute insignificantly to the overall bit error ratio when compared to an equidistant PAM-4 eye where each eye contributes a third of the errors. This property can be exploited to improve the BER in links where this transmitter is paired with a noise limited receiver.

However, if the receiver is limited in dynamic range, we could increase α (from 33% to 40% in Fig. 3(c)) to pre-distort the multilevel signal by increasing the relative eye height of the outer eyes. This way we can compensate compression in a transimpedance amplifier (TIA) or a limited analog-to-digital converter range, relaxing the linearity requirements on the receiver frontend.

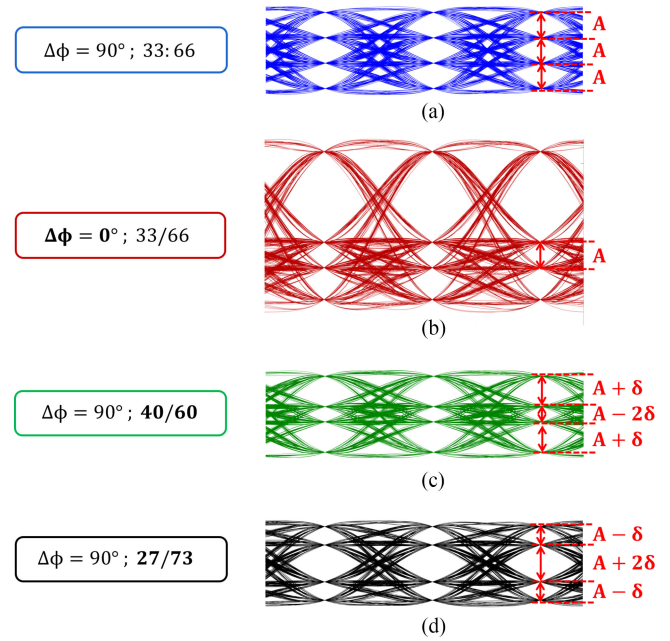


Fig. 3. Comparison of different PAM-4 shaping through vector addition by altering the phase difference or the split ratio or with respect to for equidistant PAM-4 generation with $\Delta\phi = 90^\circ$ and 0.33:0.66 split ratio.

On the other hand, reducing α will introduce the inverse effect: the inner eye height increases and the outer eye heights decrease as shown in Fig. 3(d). This type of non-uniform PAM-4 can be beneficial in flexible passive optical networks with a spread in received optical powers to increase the aggregated capacity of the network, as was recently demonstrated in [20]. Switching between different PAM-4 shapings can be done with little extra complexity by implementing a tunable splitter (e.g., by using low-power thermal phase shifters in a Mach-Zehnder Interferometer (MZI) configuration) and a tunable phase shifter between the branches the (e.g., thermal phase shifter). This way, each parameter can be changed on the fly by adjusting only a single DC voltage, accommodating many different applications without having to change the transmitter design.

III. EXPERIMENT SETUP

To verify the operation and the performance of the proposed topology, a prototype transmitter was fabricated in imec's silicon photonics platform with two standard 1×2 -MMIs as splitter and combiner, a thermal heater in each arm acting as a DC phase shift and 2 identical $80 \mu\text{m}$ long GeSi EAMs. These are the same EAMs as were used in [6] and more details on a similar but shorter EAM can be found in [19], [20]. Two 50Ω resistors are provided on-chip to allow the transmitter to be driven by an external 50Ω -driver (RF Amp) with minimal reflection. These resistors are not necessary for the operation of the transmitter and can easily be omitted when integrated with a dedicated driver. Although the operational wavelength of the GeSi EAMs in [19], [20] red shifts approximately 0.8 nm per Kelvin due to the change in bandgap, no temperature control was needed during the experiments as these devices have a 1 dB transmitter penalty bandwidth of >30 nm. Light is coupled in and out the photonic die through fiber-to-chip grat-

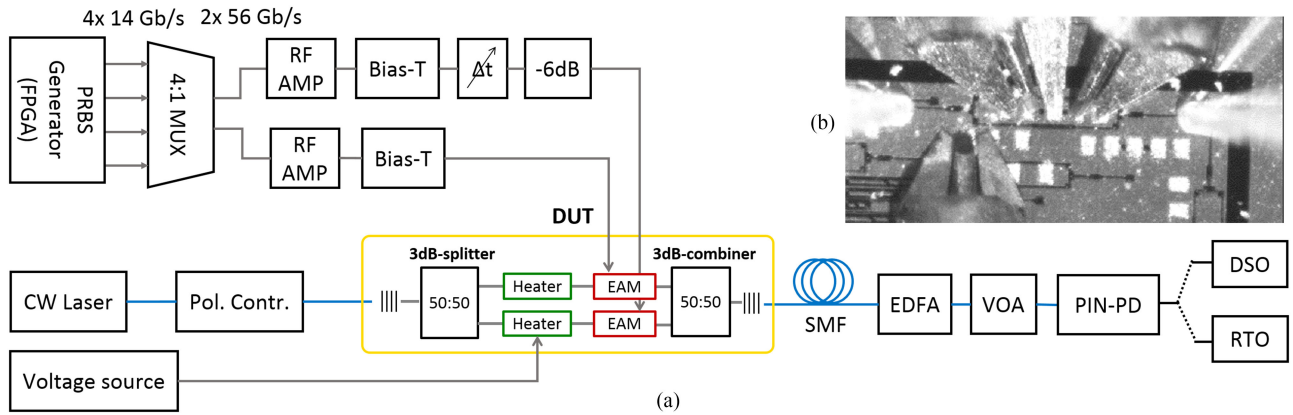


Fig. 4. (a) Experiment setup; (b) micrograph of die during experiments.

ing couplers ($IL \sim 6$ dB/coupler). As this structure does not have an optimized power splitting ratio between both EAMs, we mimic this effect by reducing the electrical swing on the LSB-arm with a 6 dB attenuator and by further increasing the bias voltage of the LSB-EAM. As a consequence, we suffer an additional insertion loss with respect to an optimized splitting ratio. Nevertheless, this operation allows us to validate the proposed transmitter topology.

The setup for transmission experiments is shown in Fig. 4. A laser source at 1577 nm with an in-fiber power of 12 dBm is coupled to the PAM-4 transmitter through fiber-to-chip grating couplers. An FPGA delivers four $2^7 - 1$ long pseudo-random bit sequences (PRBS) at 14 Gb/s to an in-house developed 4-to-1 multiplexer, which generates a differential 56 Gb/s NRZ signal. To ensure decorrelation between both signals, a tunable time delay is placed after one of the differential outputs. For these first transmission experiments at 112 Gb/s only a relatively short PRBS sequence was used. Operation with longer PRBS was investigated up to 50 GBaud with an arbitrary waveform generator (AWG) as driver. Although the performance was limited by the bandwidth of the AWG (~ 32 GHz), no eye penalty was observed for sequence up to $2^{15} - 1$ (i.e., the longest possible PRBS that could be generated by the AWG due to its limited memory).

Next, a 50 GHz RF amplifier is added to provide a swing of ~ 2.2 Vpp and ~ 1.1 Vpp to the MSB and LSB EAM, respectively. The EAMs are biased at -0.7 V and -1.8 V through internal bias-Ts in the RF amplifier. The modulators have an estimated IL and a dynamic ER of approximately 7 dB. The average optical in-fiber power after the modulator was approximately -10 dBm. A voltage source was used to introduce a 90° phase shift between both arms. As no TIA with sufficient bandwidth (i.e., >40 GHz) was available, an erbium-doped fiber amplifier (EDFA) is used to compensate the insertion losses of the grating couplers and produce sufficiently large voltage swing at the output of a commercial 50 GHz photodiode (responsivity ~ 0.65 A/W). Although the GeSi EAMs perform slightly better around 1560 nm in terms of ER per IL [20], a longer wavelength was chosen as we only had an L-band EDFA at our disposal during the experiments. In future implementations, the EDFA can be removed from the link by incorporating a linear TIA after the photodiode and by replacing the grating

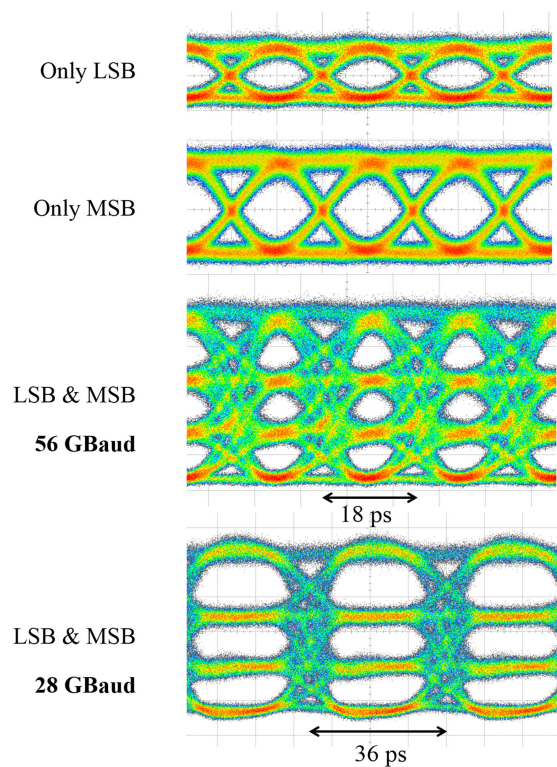


Fig. 5. Example of the received optical eyes from the prototype transmitter with only the top or the bottom EAM driven, and with both EAMs driven at 56 GBaud (112 Gb/s) and at 28 GBaud (56 Gb/s) for comparison.

couplers with low-loss edge couplers ($IL \sim 1$ dB/coupler). In the current setup, an optical modulation amplitude (OMA) of approximately 10 dBm was measured, which would correspond to an OMA of 0 dBm in an implementation with edge-couplers (gaining ~ 10 dB in power budget), but without the EDFA (losing ~ 20 dB in power budget). Moreover, the addition of a TIA should improve the signal-to-noise ratio in the link further by dropping the 50Ω termination on the PD and by eliminating the amplified spontaneous noise generated in the EDFA, as there was no optical bandpass filter present in the link to minimize this noise source. Next, a variable optical attenuator (VOA) is used to fix the average input power to the photodiode to ~ 8 dBm.

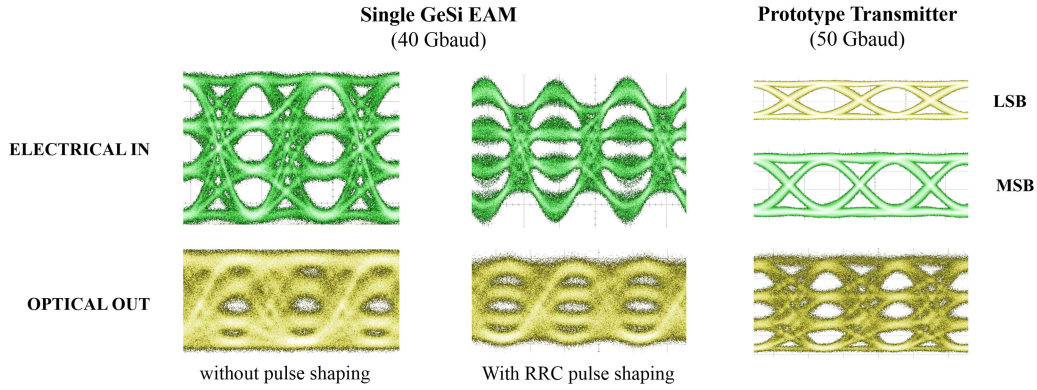


Fig. 6. Comparison of the electrical input (top) and optical output (bottom) eyes between the multilevel driven single GeSi EAM (left) and the prototype transmitter based on the proposed topology in this work (right).

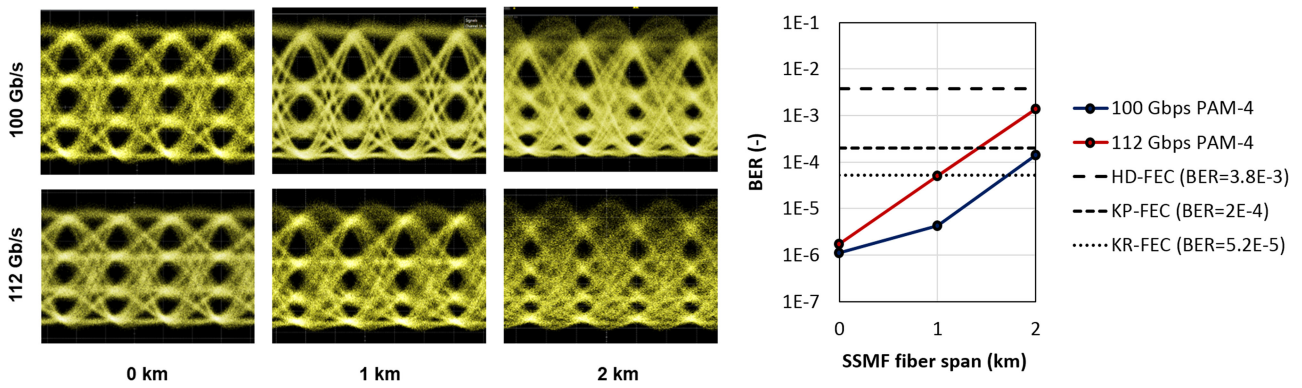


Fig. 7. Received eye diagrams and recorded BERs for 50 GBaud and 56 GBaud PAM-4 over 0, 1 and 2 km of SSMF.

Finally, the signal is captured by a 50 GHz sampling oscilloscope (DSO) for eye diagrams or stored by a 63 GHz 160 GSa/s real-time oscilloscope (RTO) for offline error counting. Due to the lack of a real-time PAM-4 analyzer, the BER is determined by resampling the stored signal and choosing the optimal sampling time and decision thresholds. To ensure a statistically relevant measurement, the captured waveform length was increased to produce at least 10 errors. Next, this four-level signal is de-mapped using Gray-coding and compared to the original transmitted bit streams. No other offline DSP or equalization was used during the error counting.

IV. RESULTS AND DISCUSSION

The DAC operation of the prototype transmitter is verified by first driving each EAM separately in order to produce the LSB and the MSB as 56 Gb/s NRZ streams, for which the resulting optical eyes are shown in Fig. 5. Next, both modulators are driven simultaneously to generate the multilevel signal. The DC phase shift needed to be adjusted slightly to compensate any residual phase difference between both branches, e.g., due to an unbalanced non-zero average phase shift by operating the EAMs at different bias voltages. Nevertheless, a high-quality PAM-4 signal with clear open eyes could be generated fairly easily at 56 Gb/s and at 112 Gb/s (Fig. 5).

To validate the assumption that an optical DAC should have a better performance than an electrical DAC scheme as it bypasses the linearity requirements at the transmitter, a single, but identical GeSi EAM is driven with a four-level signal by a 92 GSa/s AWG. Fig. 6 shows the electrical input and the optical outputs for the single modulator and for the prototype transmitter (also driven by the AWG to make a fair comparison). Even with the addition of a root-raised cosine (RRC) pulse shape by the electrical DAC, the optical DAC operation clearly outperforms a single, multilevel driven modulator.

Next, we conducted BER measurements after 0, 1 and 2 km of standard single-mode fiber at 50 and 56 GBaud, for which the received eyes and the corresponding BERs are given in Fig. 7. For 50 GBaud, we recorded BERs of $1.12\text{E-}6$ (0 km), $4.24\text{E-}6$ (1 km) and $1.4\text{E-}4$ (2 km). For 56 GBaud, we obtained BERs of $1.71\text{E-}6$ (0 km), $5\text{E-}5$ (1 km) and $1.43\text{E-}3$ (2 km). All BERs are well below the hard-decision forward error coding limit (HD-FEC) with 7% overhead of $3.8\text{E-}3$, which is often used in literature to compare devices. However, in data center applications more stringent FECs apply, such as the KP4-FEC (BER of $2\text{E-}4$) and the KR4-FEC (BER of $5.2\text{E-}5$) [1]. Nevertheless, sub-FEC operation for both the KR4- and the KP4-FEC is achieved up to 1 km at 56 GBaud. At 50 GBaud, the KP4-FEC can be supported up to 2 km. The fairly large increase in BER for longer fiber spans can be largely contributed to the relatively high chromatic dispersion (CD) at 1577 nm. As we discussed in our previous

work on the NRZ modulation of the EAM [6], the frequency response of the fiber channel in combination with the GeSi EAM as transmitter at 1560 nm has a frequency notch around 42 GHz for 2 km of SSMF, which leads to a ~ 2 dB penalty around 30 GHz. At 1577 nm, this notch will be at a lower frequency due to the higher CD, degrading the performance even further. Accounting for the lower CD and the improved performance of the GeSi EAMs at 1560 nm, as discussed in Section III, operation below the KP4-FEC limit up to 2 km should be feasible by shifting the wavelength to 1560 nm.

An additional benefit of using GeSi EAMs as amplitude modulators in the proposed transmitter topology, is that the same device can also be used as photodiode. Although such a link was not attempted in this experiment, we already demonstrated that these GeSi EAMs are capable of receiving 100 Gb/s NRZ with a responsivity close to 1 A/W [6].

Furthermore, the proposed transmitter as a whole could be used as a differential photodiode by setting the phase $\Delta\phi = 180^\circ$ and the split ratio to 50:50, i.e., a conventional 3 dB-coupler. Differential PDs are commonly used in combination with differential TIAs in coherent transceivers [21], [22], offering advantages over single-ended receivers such as a superior common-mode noise rejection and better linearity through cancellation of even-order distortion products. In many cases single-input TIAs are already designed to be fully differentially, but are made single-ended by adding a dummy load or photodiode to one of the differential inputs or by generating a differential current on-chip. In combination with the parallel EAM structure acting as a differential PD, such TIAs would require minimal effort to be converted in a truly differential optical receiver. In both cases, a compact, low-cost and low-power transceiver in silicon photonics based on a single active device as building block could be realized.

V. CONCLUSION

We have proposed a novel type of optical DAC to generate PAM-4, based on the vector addition of two binary driven amplitude modulators in parallel. A silicon prototype was fabricated using two GeSi EAMs, outperforming a single, multilevel driven GeSi EAM and demonstrating successful transmission over 2 km of SSMF up to 112 Gb/s. This is the first silicon-based modulator capable of generating 112 Gb/s PAM-4 without relying on power-hungry DSP, electrical DACs or long travelling wave structures and dedicated terminations. These results further showcase the benefit of postponing the DAC operation to the optical domain, as well as the bright future for SiP towards realizing compact, low-cost and low-power 400 GbE transceivers for short-reach optical interconnects.

REFERENCES

- [1] IEEE P802.3bs 400 Gigabit Ethernet Task Force, Jul, 15, 2017. [Online]. Available: <http://www.ieee802.org/3/bs/>
- [2] J. Lee *et al.*, "Serial 103.125-Gb/s transmission over 1 km SSMF for low cost, short-reach optical interconnects," in *Proc. Opt. Netw. Commun. Conf.*, San Francisco, CA, USA, 2014, pp. 1–3.

- [3] M. Verplaetse *et al.*, "Real-time 100 Gb/s transmission using three-level electrical duobinary modulation for short-reach optical interconnects," *J. Lightw. Technol.*, vol. 35, no. 7, pp. 1313–1319, Apr. 2017.
- [4] H. Zwickel *et al.*, "100 Gbit/s serial transmission using a silicon-organic hybrid (SOH) modulator and a duobinary driver IC," in *Proc. Opt. Fiber Commun. Conf. Exhib.*, Mar. 2017, pp. 1–3.
- [5] P. Groumas *et al.*, "Tunable 100 Gbaud transmitter based on hybrid polymer-to-polymer integration for flexible optical interconnects," *J. Lightw. Technol.*, vol. 34, no. 2, pp. 407–418, Jan. 2016.
- [6] J. Verbist *et al.*, "Real-time 100 Gb/s NRZ and EDB transmission with a GeSi electro-absorption modulator for short-reach optical interconnects," *J. Lightw. Technol.*, Nov. 20, 2017, doi: [10.1109/JLT.2017.2775630](https://doi.org/10.1109/JLT.2017.2775630).
- [7] A. Chiuchiarelli *et al.*, "Single Wavelength 100G real-time transmission for high-speed data center communications," in *Proc. 2017 Opt. Fiber Commun. Conf. Exhib.*, Los Angeles, CA, USA, 2017, pp. 1–3.
- [8] Q. Zhang *et al.*, "Single-lane 180 Gb/s SSB-duobinary-PAM-4 signal transmission over 13 km SSMF," in *Proc. 2017 Opt. Fiber Commun. Conf. Exhib.*, Mar. 2017, pp. 1–3.
- [9] D. Patel, A. Samani, V. Veerasubramanian, S. Ghosh, and D. V. Plant, "Silicon photonic segmented modulator based electro-optic DAC for 100 GB/s PAM-4 generation," *IEEE Photon. Technol. Lett.*, vol. 27, no. 23, pp. 2433–2436, Dec. 2015.
- [10] A. Samani *et al.*, "A silicon photonic PAM-4 modulator based on dual-parallel Mach-Zehnder interferometers," *IEEE Photon. J.*, vol. 8, no. 1, Feb. 2016, Art. no. 7800610.
- [11] M. Chagnon *et al.*, "Duobinary IQ modulation schemes for C- and O-band PAM4 direct detect systems," in *Proc. Eur. Conf. Opt. Commun.*, 2017, pp. 1–3.
- [12] R. Li *et al.*, "An 80 Gb/s silicon photonic modulator based on the principle of overlapped resonances," *IEEE Photon. J.*, vol. 9, no. 3, Jun. 2017, Art. no. 4900311.
- [13] R. Lui *et al.*, "Silicon photonic ring-assisted MZI for 50 Gb/s DAC-less and DSP-free PAM-4 generation," *IEEE Photon. Technol. Lett.*, vol. 29, no. 12, pp. 1046–1049, Jun. 2017.
- [14] A. Abbasi *et al.*, "III-V-on-silicon C-band high-speed electro-absorption modulated DFB laser," *J. Lightw. Technol.*, Aug. 25, 2017, doi: [10.1109/JLT.2017.2743044](https://doi.org/10.1109/JLT.2017.2743044).
- [15] Huang *et al.*, "Optical DAC for Generation of PAM4 using parallel electro-absorption modulators," in *Proc. 42nd Eur. Conf. Opt. Commun.*, Dusseldorf, Germany, 2016, pp. 1–3.
- [16] M. Theurer *et al.*, "2 × 56 Gb/s From a double side electroabsorption modulated DFB laser and application in novel optical PAM4 Generation," *J. Lightw. Technol.*, vol. 35, no. 4, pp. 706–710, Feb. 2017.
- [17] J. Verbist *et al.*, "DAC-less and DSP-free PAM 4 transmitter at 112 Gb/s with two parallel GeSi electro-absorption modulators," in *Proc. Eur. Conf. Opt. Commun.*, 2017, paper Th.PDP.C.5.
- [18] R. van der Linden *et al.*, "Improvement on received optical power based flexible modulation in a PON by the use of non-uniform PAM," in *Proc. Eur. Conf. Opt. Commun.*, 2017, pp. 1–3.
- [19] M. Pantouvaki *et al.*, "Active Components for 50 Gb/s NRZ-OOK optical interconnects in a silicon photonics platform," *J. Lightw. Technol.*, vol. 35, no. 4, pp. 631–638, Feb. 2017.
- [20] S. A. Srinivasan *et al.*, "50 Gb/s C-band GeSi Waveguide electro-absorption modulator," in *Proc. 2016 Opt. Fiber Commun. Conf. Exhib.*, Mar. 2016, paper Tu3D.7.
- [21] A. Awny *et al.*, "A linear differential transimpedance amplifier for 100-Gb/s integrated coherent optical fiber receivers," *IEEE Trans. Microw. Theory Techn.*, Sep. 28, 2017, doi: [10.1109/TMTT.2017.2752170](https://doi.org/10.1109/TMTT.2017.2752170).
- [22] J. S. Weiner *et al.*, "SiGe differential transimpedance amplifier with 50-GHz bandwidth," *IEEE J. Solid-State Circuits*, vol. 38, no. 9, pp. 1512–1517, Sep. 2003.

Authors' biographies not available at the time of publication.